

# Light propagation in ERL bunch length measurements

Michael Gerrity

*Department of Physics, University of Texas at Austin, Austin, Texas, 78705*

(Dated: August 11, 2005)

Terahertz radiation can be used to determine the bunch shape of an electron bunch in an accelerator. Beamlines are often used to transport this radiation away from the accelerator to a shielded detector for analysis. The current beamline at the Jefferson Free Electron Laser as well as several variants are analyzed to compare their relative diffraction losses, which are found to be quite minimal. The transmission of light pipes are also analyzed as a possible alternative to beamlines and are found to have significant, but not prohibitive, energy losses.

## I. INTRODUCTION

An electron bunch in an accelerator can have instabilities in its configuration that propagate over time and reduce the operating efficiency of the accelerator. Knowledge of the shape of an electron bunch allows these instabilities to be detected so that the accelerator may be tuned to minimize them. The shape of an electron bunch can be determined by measuring the intensity spectrum of the coherent radiation in the far infrared (Terahertz) region. For a bunch of  $N$  electrons, the intensity of coherently emitted radiation is proportional to  $N^2$ , while the intensity of incoherent radiation is directly proportional to  $N$ . This amplification eases the measurement of the intensity spectrum and thus allows for a more accurate determination of the bunch shape.

Even so, various factors can hamper an accurate measurement of the intensity spectrum. As the high X-ray levels near an accelerator can damage a THz detector, the detector must be placed in a shielded location spatially separated from the accelerator. Most often a beamline is used to relay the THz radiation from the accelerator to the detector. Spatially separating the detector from the accelerator allows energy to be lost due to diffraction. In addition the beamline itself can act as a low frequency cutoff. This paper analyzes the diffraction losses of the beamline at the Jefferson Free Electron Laser and several variations upon this design as well as the losses of simpler beamlines and light pipes.

## II. BACKGROUND THEORY

<sup>1</sup> It is known that a single electron has an intensity spectrum  $I(\omega)$  proportional to the square electric field  $E$ ,

$$I(\omega) \propto |E|^2. \tag{1}$$

This can be extended to the case of a bunch of particles emitting coherently at a distance  $R$  from the detector, where  $R$  is much greater than the size of the bunch. The total intensity

---

<sup>1</sup> The derivation in this section closely follows that in [1]

spectrum seen by the detector is found to be

$$I_{tot}(\omega) = I(\omega) \left| \sum_{j=1}^N e^{i(\omega/c)\mathbf{n}\cdot\mathbf{r}_j} \right|^2, \quad (2)$$

where  $\mathbf{r}_j$  is the location of the  $j$ th charge and  $\mathbf{n}$  is a unit vector pointing to the  $j$ th charge. This can be rewritten by expanding the double sum

$$I_{tot}(\omega) = I(\omega) \left( N + \sum_{j \neq k}^N e^{i(\omega/c)\mathbf{n}\cdot(\mathbf{r}_k - \mathbf{r}_j)} \right). \quad (3)$$

Taking the average of the bracketed term with respect to position and assuming the particles are uncorrelated gives a relation between the intensity spectrum and the form factor  $F(\omega)$ .

$$I_{tot}(\omega) = I(\omega) [N + N(N-1)F(\omega)] \quad (4)$$

$$F(\omega) = \left| \int d\mathbf{r} S(\mathbf{r}) e^{i(\omega/c)\mathbf{n}\cdot\mathbf{r}} \right|^2. \quad (5)$$

By substituting the longitudinal particle distribution  $S(z)$  in for  $S(\mathbf{r})$

$$S(z) = \int_{\perp} S(\mathbf{r}) dx dy, \quad (6)$$

we relate the form factor to the longitudinal distribution

$$F(\omega) = \left| \int_{-\infty}^{\infty} dz S(z) e^{i(\omega/c)z} \right|^2. \quad (7)$$

By assuming the bunch is symmetric about  $z = 0$ ,  $S(z)$  can be solved for with the inverse Fourier transform of  $F(\omega)$

$$S(z) = \frac{1}{\pi c} \int_0^{\infty} d\omega \sqrt{F(\omega)} \cos\left(\frac{\omega z}{c}\right). \quad (8)$$

While this works well for a symmetric bunch there is no reason why the bunch must be symmetric; using this method any information about any bunch asymmetry will be lost. In addition, this demands that the maximum of the longitudinal distribution be at  $z = 0$ , which does not have to be the case, even if the bunch is symmetric about  $z = 0$ . It's easy to imagine a dumbbell shaped bunch with a local minimum at  $z = 0$ .

Another method of analysis can be used by which both the phase and the amplitude of the form factor are found, which allows for the shape of asymmetric bunches to be calculated as well. Define

$$\hat{S}(\omega) \equiv \int_0^{\infty} dz S(z) e^{i(\omega/c)z} \equiv \rho(\omega) e^{i\psi(\omega)}, \quad (9)$$

by which

$$F(\omega) = S(\omega) S^*(\omega) = \rho^2(\omega). \quad (10)$$

Taking the natural log of  $\hat{S}(\omega)$

$$\ln \hat{S}(\omega) = \ln \rho(\omega) + i\psi(\omega), \quad (11)$$

allows a Kramers-Kronig relation to be written for the real and imaginary parts in the form of a minimal phase  $\psi_m(\omega)$  and a Blaschke product  $\psi_{Blaschke}(\omega)$

$$\psi_m(\omega) + \psi_{Blaschke}(\omega) = -\frac{2\omega}{\pi}PV \int_0^\infty dx \frac{\ln \rho(x)}{x^2 - \omega^2} + \sum_j \arg \left( \frac{\omega - \hat{\omega}_j}{\omega - \hat{\omega}_j^*} \right), \quad (12)$$

where the  $\hat{\omega}_j$ 's are the zeros of  $\hat{S}(\omega)$  in the upper half of the complex plane.

In general the Blaschke product can not be determined, but there are certain special cases in which it can be neglected. As zeroes along the real axis make an insignificant contribution to the total sum, and Titchmarsh's Theorem shows that as the real axis goes to infinity the zeroes tend towards the real axis, only zeros close to where the intensity spectrum is measured have any effect on the phase. If there are no nearby zeroes the Blaschke product can be ignored and the minimal phase as seen in Eqn. 12 is a good approximation for the total phase. Adding

$$-\frac{2\omega}{\pi}PV \int_0^\infty dx \frac{\ln \rho(\omega)}{x^2 - \omega^2} = 0, \quad (13)$$

to Eqn. 12 removes the singularity at  $x = \omega$ , and the minimal phase is found to be

$$\psi_m(\omega) = -\frac{2\omega}{\pi} \int_0^\infty dx \frac{\ln [\rho(x)/\rho(\omega)]}{x^2 - \omega^2}. \quad (14)$$

Having measured the form factor directly, and thus knowing  $\rho(\omega)$ , the inverse Fourier transform of Eqn. 9 gives the longitudinal bunch distribution,  $S(z)$ ,

$$S(z) = \frac{1}{\pi c} \int_0^\infty d\omega \rho(\omega) \cos \left[ \psi_m(\omega) - \frac{\omega z}{c} \right]. \quad (15)$$

### III. ZEMAX

The optical engineering program ZEMAX was used to model and analyze the current JFEL beamline as well as several variations. In ZEMAX optical designs are modelled by specifying surfaces. Creating a simple thin glass lens requires specifying two surfaces; the front and back faces. ZEMAX can be used in two modes: sequential and non-sequential. In sequential mode, surfaces are created in a definite order; light interacts with each surface once and only once, and after interacting with a surface ZEMAX will propagate the light until it strikes the next listed surface. Any surfaces between the two are ignored in the propagation. In non-sequential mode, light can interact with any surface any number of times, in any order. ZEMAX launches beams from specified light sources, which are then propagated until they either diverge (in which case they are dropped) or they strike a surface. Upon striking a surface the light is either refracted or reflected according to the rules of geometrical optics.

ZEMAX uses both ray tracing and physical optics propagation, although physical optics propagation can only be used in the sequential mode. Since diffraction effects can only be calculated using physical optics, the vast majority of the analysis was done in sequential mode. Light pipes were modelled in non-sequential mode, as the light can strike a single surface multiple times. While this doesn't allow for the calculation of any diffraction effects, such losses are so small as to be negligible in light pipes.

Beamlines modelled in ZEMAX were tested for a variety of wavenumbers, ranging from  $5\text{cm}^{-1}$  to  $120\text{cm}^{-1}$  in increments of  $5\text{cm}^{-1}$ .

#### IV. JFEL BEAMLINE

The current beamline at JFEL is shown in Fig. 1. Synchrotron radiation is emitted by an electron bunch approximately 3mm horizontal by 2mm vertical in size. The light is about 60% vertically polarized, the rest horizontally polarized. The source emits the radiation into a subtended angle of about 200 milliradians horizontal by 135 milliradians vertical.

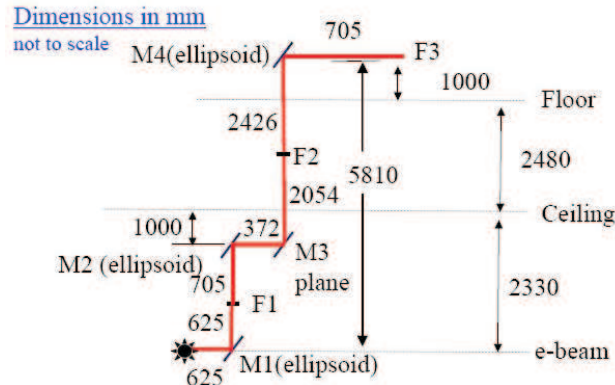


FIG. 1: The current design of the JFEL beamline.

After being emitted, the light is reflected off of four mirrors, three ellipsoidal and one planar. All of the mirrors are made of polished aluminum and about 150mm in diameter. There are two intermediate focal points before the final focus at the detector. A diamond window 20mm in diameter is located at F1, separating the  $1 \times 10^{-9}$  Torr vacuum in the accelerator from the 100 millitorr vacuum in the beamline.

Several variants of the current JFEL beamline were also tested. Most of the designs tested had the same physical configuration as the current beamline, using four mirrors of the same size in the same locations as in the present design. Among the variations tested were beamlines with three intermediate focal points, beamlines using parabolic and planar mirrors to send a collimated beam through the beamline until the final focus, as well beamlines implementing a combination of both ellipsoidal and parabolic mirrors allowing for both focused and collimated stretches. The possibility of using beamlines with only two mirrors was also considered. These designs were based upon an entirely different physical layout than the current design. Only two such designs like this were tested, one using a collimated beam and the other using a focused beam.

Ellipsoidal mirrors are used to create beamlines with multiple intermediate focal points. Much like an ellipse, all light emitted from one focal point of an ellipsoid is focused at the other focal point. There are a few advantages to using ellipsoidal mirrors and several intermediate focal points. Focal points are very convenient if a change in pressure is desired, as a window placed at the focal point need not be as big as it would have to be if placed elsewhere along the beamline. The biggest disadvantage of using ellipsoidal mirrors is their lack of versatility. The only way these mirrors can be reused should the beamline be modified in the future is if there is a need for a mirror with the exact same focal lengths.

A parabolic mirror will take all the light emitting from its focal point and collimate it. Conversely, it will take all light from an incident beam of parallel light and focus it at the focal point. As a beam, once collimated, will stay that way (for our purposes), it doesn't matter at what distance the next mirror is placed. This allows for much greater versatility

than ellipsoidal mirrors. It is far easier to reuse a parabolic mirror than an ellipsoidal mirror should the need arise.

## V. BEAMLINER RESULTS

After calculating the diffraction losses and variance with position of each four-mirror design in ZEMAX, it was found that all of the designs tested performed very well in both minimizing diffraction losses and maintaining uniform diffraction losses. The average transmission and variance in transmission with position for each beamline tested are shown in Table I.

TABLE I: Transmission and variance with position of tested beamlines

Beamline	Transmission	Variance
Current JFEL Beamline	.999294	$3.25 \times 10^{-4}$
Collimated Beamline	.991440	$6.32 \times 10^{-4}$
Three-Focus Beamline	.999322	$9.29 \times 10^{-5}$
PC2	.991148	$7.58 \times 10^{-4}$
PC3	.999021	$6.55 \times 10^{-5}$
PC4	.999330	$3.14 \times 10^{-4}$
TM Focused	.999275	$3.08 \times 10^{-4}$
TM Collimated	.999139	$6.55 \times 10^{-4}$

As can be seen, the current beamline performs very well; on average less than 0.1% of the total energy is lost to diffraction with an average variation with position less than .05%. Compared to the current beamline, only the three-focus design and PC4 performed better in both categories. PC3 had slightly lower transmission and more uniform losses. Both PC2 and the collimated design performed worse in both categories. As both of these designs had a collimated beam in between M1 and M2, the window at F1 blocks some of the incident radiation, especially at higher wavelengths where on order of 10% of the energy was sometimes lost. This accounts for these two designs having significantly lower transmission than the designs with a focus at F1. The transmission at each wavenumber tested for the four-mirror designs are seen in Fig. 2.

It is important to note that the two-mirror beamlines can not be directly compared to the four-mirror designs. As the two-mirror designs use an entirely different physical layout than that of the four-mirror designs, the two-mirror designs are advantaged in their analysis in that they do not have the window at F1 possibly absorbing radiation. While any two-mirror design that was actually constructed would most certainly use a window somewhere, the window could be put in any number of places. For this reason the two-mirror beamlines were tested in the absence of any window.

That said, the two-mirror beamlines can be compared against the four-mirror beamlines, so long as it is remembered that any comparison is slightly flawed. It was found that the two-mirror designs performed on par with the four-mirror designs. The focused design was found to perform better than the collimated design in both minimizing losses due to diffraction and maintaining uniform losses. Compared to the current beamline, the focused design was

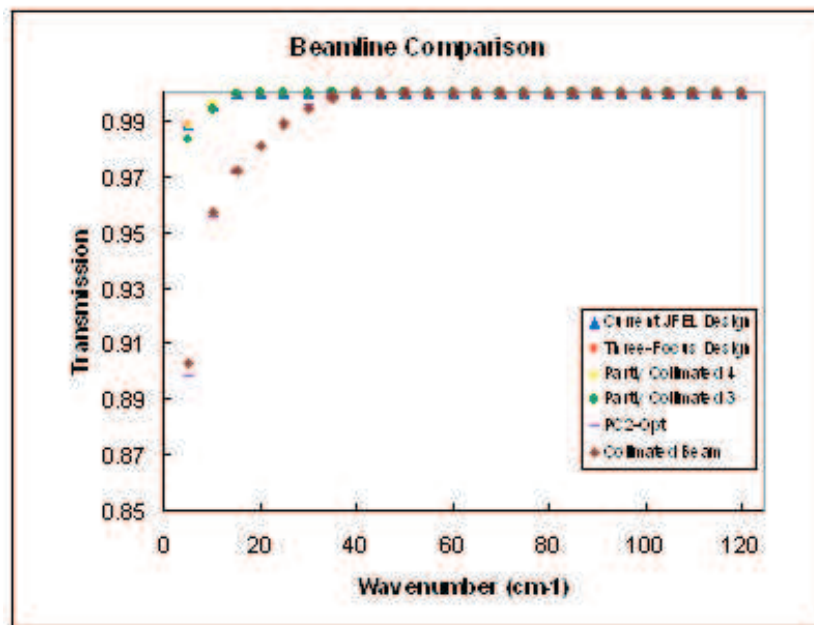


FIG. 2: Fraction of energy lost due to diffraction for four-mirror beamlines

found to have a slightly lower average transmission, but slightly more uniform losses. The transmission at each wavelength for both of the two-mirror beamlines are shown in Fig. 3.

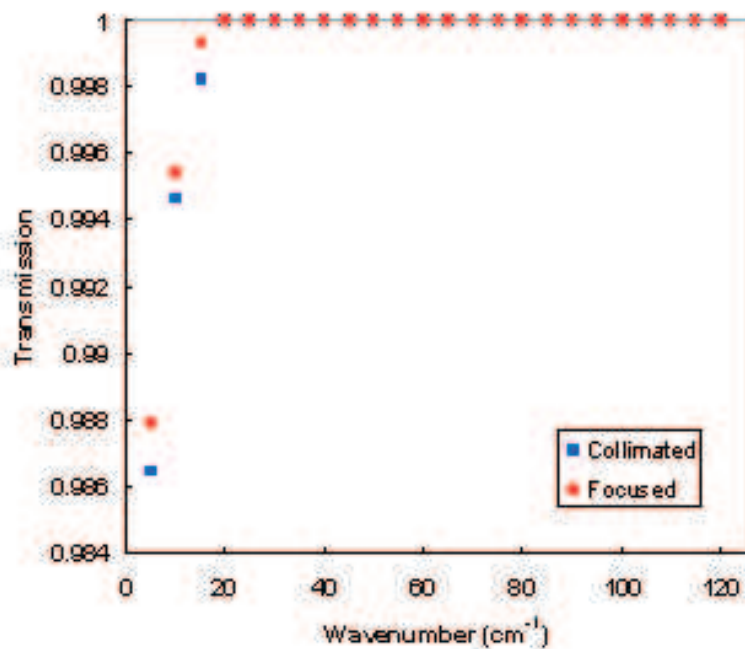


FIG. 3: Fraction of energy lost due to diffraction for two-mirror beamlines

## VI. LIGHT PIPE RESULTS

In addition to beamlines, light pipes were also considered. A light pipe is a metal tube that uses reflection to transport light from one place to another. A light pipe has several potential advantages over a beamline. Light pipes are much smaller than beamlines, so they take up less laboratory space. Light pipes are also much less expensive than a beamline. Whereas a beamline can run anywhere from \$10,000 to \$100,000, a light pipe can be used for less than \$1,000. The combination of size and price allows using multiple light pipes at successive locations along the accelerator to monitor the evolution of the bunch shape. As for disadvantages, the first is that the transmission of a light pipe is not as high as that of a beamline. Secondly, the frequency ranges that can be transmitted by a light pipe are much smaller than that of a beamline.

Creating a light pipe in ZEMAX required defining a coating by specifying the real and complex indices of refraction at the needed wavelengths. These were calculated for brass using the Drude model of metals. In the Drude model, the dielectric function of a metal,  $\epsilon(\omega)$ , is defined by

$$\epsilon(\omega) = 1 - \frac{\omega_{pl}^2}{\omega(\omega + i\Gamma)}, \quad (16)$$

where  $\omega_{pl}$  is the plasma frequency defined by

$$\omega_{pl}^2 = \frac{4\pi n_e e^2}{m_e}. \quad (17)$$

In the above  $n_e$  is the carrier density, and  $m_e$  and  $e$  are the mass and charge of an electron, respectively. In the dielectric function  $\Gamma = 1/\tau$ , where  $\tau$  is the relaxation time,

$$\tau = \frac{m_e}{\rho n_e e^2}, \quad (18)$$

and  $\rho$  is the electrical resistivity. From here  $\eta$  can be found, where  $\eta = n + ik$ , by noting that

$$\epsilon(\omega) = \eta^2, \quad (19)$$

and so

$$\epsilon_r(\omega) = n^2 - k^2, \quad (20)$$

and

$$\epsilon_i(\omega) = 2nk. \quad (21)$$

The values from [2] were used for  $n_e$  and  $\rho$ . The calculated values for  $n$  and  $k$  are shown in Fig. 4

Three different light pipe designs were considered, all of the same length. The first was in the same shape as the current beamline at JFEL. The second followed the shape of the two mirror beamlines, and the third was a simple straight pipe to help see the effects of elbows on transmission. All of the light pipes had a radius of 25mm, and they all began 300mm from the source of the light. The electron bunch was modelled using a point source emitting into a cone with a half angle of 1.5°.

To analyze a light pipe, a detector was placed at the end of the light pipe and rays were randomly launched from the source into a cone, which were then propagated through the light pipe until they reached the detector and were absorbed, or dropped below a certain

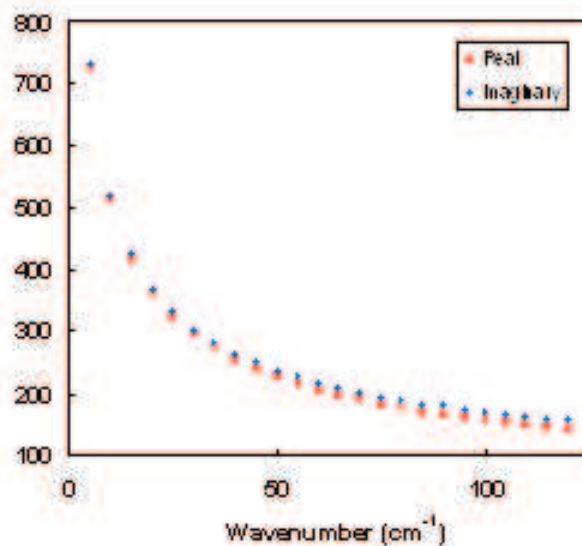


FIG. 4: Real and imaginary parts of the index of refraction as calculated by the Drude model

energy and were discarded. At each interaction ZEMAX calculated the amount of energy reflected back into the light pipe and the amount which propagated out using the values specified in the coating file. The total energy that reaches the detector was recorded, which was then divided by the initial energy to find the transmission.

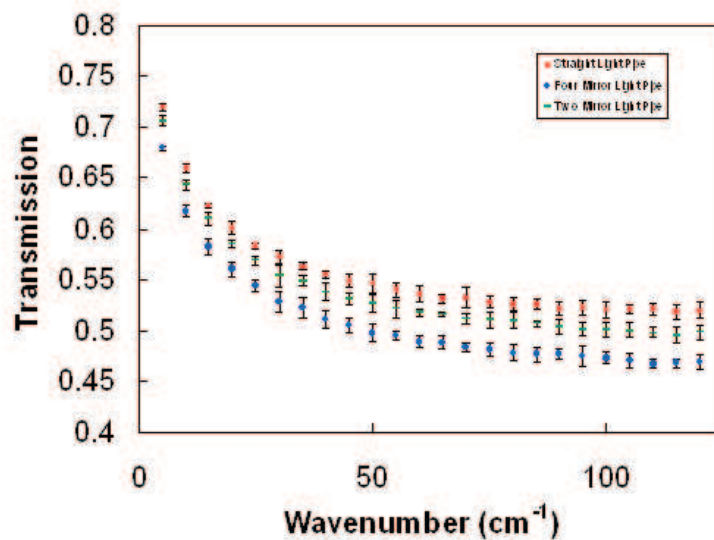


FIG. 5: Fraction of energy transmitted by light pipes

As expected, it was found that light pipes in general offer much lower transmission than do beamlines. Whereas beamlines had transmission rates well above 90%, light pipes, even at low wavenumbers where they performed best, never broke 75%. On average their trans-

mission was much closer to 50% of the total energy. Fig. 5 shows the transmission of the three light pipes at the tested wavenumbers. It can also be seen that the number of elbows very clearly affects the amount of energy transmitted, with the straight pipe giving the highest transmission, and the four-elbow pipe offering the lowest.

## VII. CONCLUSIONS

From the results obtained it can be concluded that in terms of sheer transmission and minimal variance, beamlines have performance much better than light pipes. Among the beamlines, it was found that the Three-Focus design and PC4 both performed better than the current design; given unlimited resources would probably represent the ideal choices. When the fact that a lab does not have unlimited resources is considered, the choice is much less obvious. While offering the better performance than the current design, the price tag would also be larger, as the current design uses three aspheric and one planar mirror, and these both use four aspheric mirrors. In most situations, it would probably be best to use a two-mirror beamline if possible, given the significantly reduced cost.

While light pipes offered much lower performance than beamlines, the possible benefits of using multiple light pipes and the reduced cost still make them a viable option for labs to use. When deciding whether to use a beamline or a light pipe, the lab will have to decide what level of performance is necessary for what they need and how much they're willing to spend.

## VIII. ACKNOWLEDGEMENTS

I would like to thank my mentor, Nick Agladze, for all of his help and support throughout the project. I would also like to thank Rich Galik for all that he did in helping us feel welcome here and answering our questions, as well as LEPP and Cornell University for allowing me to have this opportunity. I would also like to thank Julia Stroud for all of her help. I would lastly like to thank the NSF for funding this project and making this possible. This project was supported by the National Science Foundation REU grant PHY-0243687 and research co-operative agreement PHY-9809799.

- 
- [1] R. Lai, A.J. Sievers, Nucl. Instr. and Meth. A **397** 221-231 (1997)
  - [2] D. Miller, P.L. Richards, S. Etemad, A. Inam, T. Venkatasen, B. Dutta, X.D. Wu, C.D. Eom, T.T. Geballe, N. Newman, B.F. Cole, Phy. Rev. B **47** 8076-8088 (1993)
  - [3] D.G. Hawthorn, T. Timusk, Appl. Opt. **38** 1787-1794 (1999)